ELSEVIER

Bone 41 (2007) 775–785

BONE

www.elsevier.com/locate/bone

Enhancement of graft bone healing by intermittent administration of human parathyroid hormone (1–34) in a rat spinal arthrodesis model ☆

Yuichiro Abe [a], Masahiko Takahata [a,*], Manabu Ito [a], Kazuharu Irie [b], Kuniyoshi Abumi [a], Akio Minami [a]

[a] *Department of Orthopaedic Surgery, Hokkaido University Graduate School of Medicine, Kita-15 Nishi-7, Kita-ku, Sapporo, 060-8638, Japan*
[b] *Department of Oral Anatomy, Health Sciences University of Hokkaido School of Dentistry, Ishikari-Tobetsu, Japan*

Received 3 April 2007; revised 29 May 2007; accepted 27 June 2007
Available online 13 July 2007

Abstract

Bone grafting is commonly used to treat skeletal disorders associated with large bone defect or unstable joint. It can take several months, however, to achieve a solid union and bony fusion sometimes delays or fails especially in osteoporosis patients. Therefore, we used a rat spinal arthrodesis model to examine whether intermittent administration of human PTH(1–34) accelerates bone graft healing. Eighty-two male Sprague–Dawley rats underwent posterolateral spinal arthrodesis surgery using autologous bone grafts. Animals were given daily subcutaneous injections of hPTH(1–34) (40 μg/kg/day PTH group) or 0.9% saline vehicle (control group) from immediately after surgery till death. Five rats each were killed 2, 4, 7, and 14 days after the surgery, and mRNA expression analysis was performed on harvested grafted bone. Seven rats each were killed 14, 28, and 42 days after the surgery, and the lumbar spine, which contained the grafted spinal segment, was subjected to fusion assessment, microstructural analysis using three-dimensional micro-computed tomography, and histologic examination. Serum bone metabolism markers were analyzed.

The results indicated that PTH administration decreased the time required for graft bone healing and provided a structurally superior fusion mass in the rat spinal arthrodesis model. PTH administration increased the fusion rate on day 14 (14% in the control group and 57% in the PTH group), accelerated grafted bone resorption, and produced a larger and denser fusion mass compared to control. mRNA expression of both osteoblast- and osteoclast-related genes was upregulated by PTH treatment, and serum bone formation and resorption marker levels were higher in the PTH group than in the control group. Histologically calculated mineral apposition rate, mineralized surface and osteoclast surface were also higher in the PTH group than in the control group. These findings suggest that intermittent administration of PTH(1–34) enhanced bone turn over dominantly on bone formation at the graft site, leading to the acceleration of the spinal fusion. Based on the results of this study, intermittent injection of hPTH(1–34) might be an efficient adjuvant intervention in spinal arthrodesis surgery and all other skeletal reconstruction surgeries requiring bone grafts.

Keywords: Parathyroid hormone; Bone graft; Spinal arthrodesis surgery; Microstructural indices analysis; Bone remodeling

Introduction

Bone grafting is a commonly used procedure to treat skeletal disorders such as bone tumor, trauma, pseudoarthrosis, and destructive spine or joint diseases that are associated with bone defects. In the treatment of these diseases, bone grafts are used for the purpose of regenerating bone defects to restore the original condition of the bone or for stabilizing an unstable joint, and the estimated number of bone grafts performed each year in the United States is 500 000 [5,31]. Among various bone graft surgeries, spinal arthrodesis surgery is the most common application [5,21]. This procedure is the gold standard treatment for degenerative and traumatic spine diseases that are associated with severe neck or back pain, and sometimes neurologic problems. In this procedure, bone grafts are used to restore

☆ All funding sources supporting the publication of the study: Asahi Kasei Corp.
* Corresponding author. Fax: +81 11 706 6054.
E-mail address: takamasa@med.hokudai.ac.jp (M. Takahata).

8756-3282/$ - see front matter © 2007 Elsevier Inc. All rights reserved.
doi:10.1016/j.bone.2007.06.025

mechanical stability to the affected unstable spinal segment by providing bridging bone between vertebrae. Because successful bony fusion between unstable spinal segments leads to pain relief and neurologic recovery, the efficacy of this procedure has gained wide acceptance and the number of these types of surgery has increased annually with the increase in the aged population [8,29,43,46]. The length of time required to achieve a solid union after spinal arthrodesis surgery and the fact that fusion is sometimes delayed or even fails, especially in osteoporosis patients [14,34,44], however, remains a serious problem. Consequently, an efficient method for enhancing graft bone healing in spinal arthrodesis surgery is needed.

Intermittent administration of parathyroid hormone (PTH) has potent anabolic effects on bone remodeling [12,13]. Because intermittent PTH treatment increases bone mass and reduces the risk for osteoporotic vertebral fractures, recombinant human PTH (1–34) has already been approved as a treatment for severe osteoporosis in the United States and in European countries [16,26,33]. The results of recent animal studies suggest that intermittent administration of PTH(1–34) enhances the bone healing process. In the long bone fracture model, intermittent injection of PTH(1–34) increases the union rate, amount of callus, bone mineral density, and mechanical strength [1–3,19,24,32]. Intermittent PTH treatment also decreases the length of time needed for bone consolidation and enhances regenerated bone strength in a rat distraction osteogenesis model [38]. Therefore, we hypothesized that intermittent PTH treatment would enhance graft bone healing.

The objectives of this study were to elucidate whether intermittent administration of PTH(1–34) enhances graft bone healing and to gain insight into the effect of intermittent administration of PTH on graft bone metabolism in a rat spinal arthrodesis model.

Materials and methods

Animals and reagents

Male Sprague–Dawley rats (n=82; 8 weeks of age; CLEA Japan, Inc., Tokyo, Japan) were maintained at 20 °C on a 12-h light/12-h dark cycle with free access to water and rat food. A powdered form of human PTH(1–34) (hPTH; Asahi Kasei Corporation, Tokyo, Japan) was dissolved in saline to 40 μg/ml.

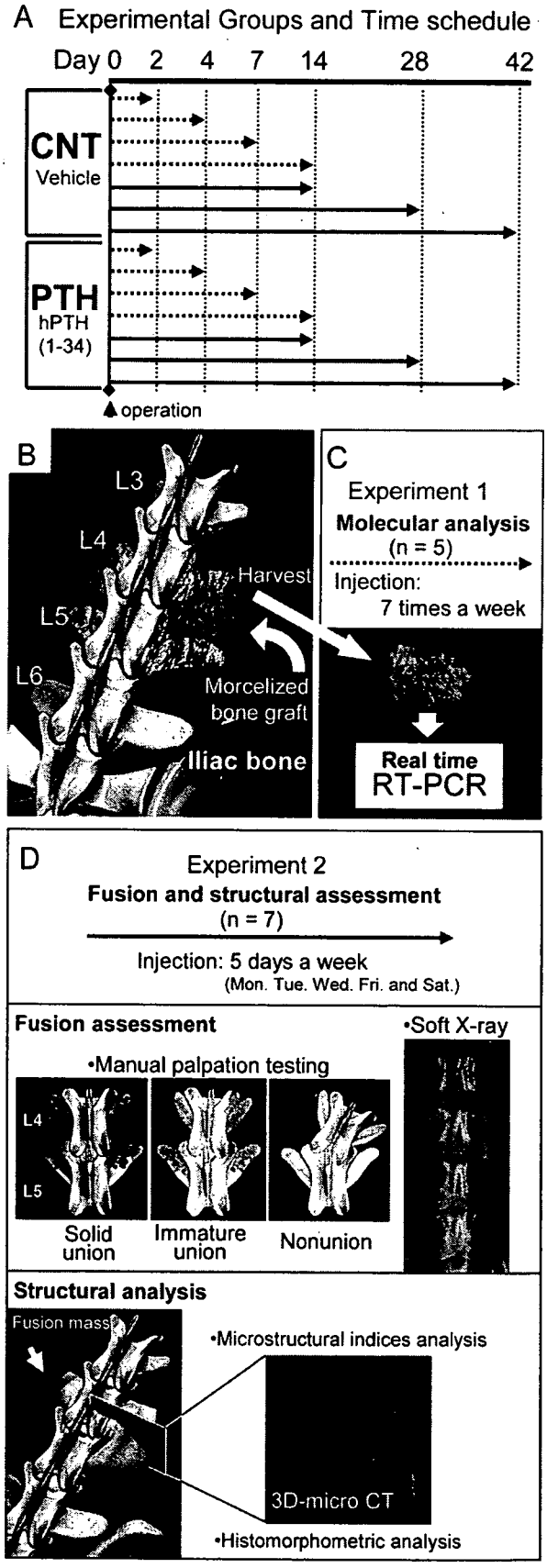

Fig. 1. (A) Experimental groups and time schedules. For Experiment 1, which was designed for molecular analysis (dotted arrow), five rats each were euthanized on days 2, 4, 7, and 14 postoperatively in both control and PTH groups. For Experiment 2, which was designed for fusion and structural assessment (arrow), seven rats each were euthanized on days 14, 28, and 42 postoperatively in both groups. (B) Schematic diagram of rat spinal arthrodesis surgery. Iliac bone was harvested and morselized graft bone was implanted in the space between the L4 and L5 transverse processes. (C) Experiment 1. Molecular analysis. Grafted bone was harvested and mRNA expression level of targeted genes was measured using real-time RT-PCR. (D) Experiment 2. Fusion and microstructural assessment. Fusion was assessed by manual palpation testing and soft X-ray observation. The L4–L5 segment was graded as a solid union when no motion was observed: immature union when bony continuity was observed between the L4 and L5 transverse processes, but the segment has slight motion, or nonunion when wide motion equivalent to adjacent segments was observed. Micro-computed tomography scanning in the axial plane was performed to evaluate the calcified fusion mass, and microstructural indices were measured from the 3D reconstruction images. Histomorphometric analysis was performed on calcein double-labeled undecalcified sections.

Experimental design

Spinal arthrodesis was surgically induced in rats at 8 weeks of age using autologous iliac bone grafts. In Experiment 1, molecular analysis was performed in the first 40 animals, and in Experiment 2, the structural fusion mass was assessed in another 42 animals (Fig. 1). The animals in each experiment were randomized into two groups; rats in the control group were given subcutaneous injections of 0.9% saline vehicle, and rats in the PTH group (PTH) were given subcutaneous injections of hPTH (40 μg/kg/day). Dosing was initiated just after surgery and continued until the rats were killed at the indicated intervals. In Experiment 1, injections were performed seven times a week and five rats of each group were killed by exsanguination of the carotid artery under general anesthesia on postoperative days 2, 4, 7, and 14 and the harvested graft bone was used for molecular analysis (Fig. 1C). In Experiment 2, injections were performed five times a week and seven rats of each group were killed on days 14, 28, and 42, and the lumbar spines, which contained the fusion segment, and the fusion mass was analyzed histomorphometrically and radiologically (Fig. 1D). All rats in Experiment 2 were double-labeled with a subcutaneous injection of calcein (10 mg/kg; Wako, Ltd., Osaka, Japan) at 9 days and 2 days before death. Before killing the animals, blood was collected and stored at −83 °C until analysis of the serum bone metabolism markers. This experimental protocol was approved by the Animal Study Committee of Hokkaido University.

Surgical procedures

Anesthesia was induced with ketamine (90 mg/kg i.p.), and maintained with isoflurane (0.5% to 2%) and oxygen using a coaxial nose cone. After shaving and prepping the surgical site, the rats were placed prone on the operating table. L4–L5 posterolateral intertransverse process arthrodesis was then performed according to Salamon with slight modification (Fig. 1B) [36]. Briefly, a posterior midline incision was made over the lumbar spine. Two paramedian fascial incisions were made 2 mm from the midline. The transverse processes of L4 and L5 vertebrae were then exposed by splitting the back muscles (Wiltse's approach). The level of arthrodesis was identified during the surgery by referencing the iliac crests. Once exposed, the transverse processes and the lateral gutters of the L4 and L5 vertebrae were decorticated with an electric bur until a blush of cancellous bone was observed. This decortication procedure at the fusion bed is a key technique in spinal arthrodesis surgery both clinically and experimentally, and therefore this procedure was performed under microscopy. Autologous bone was then harvested from the iliac crests bilaterally through the fascial incisions. A rongeur was used to harvest approximately 0.2 g of corticocancellous bone from each iliac wing. After irrigating the wound, harvested iliac bone was morselized and implanted on the decorticated fusion beds bilaterally to bridge the L4 and L5 transverse processes. The fascia and skin were closed with 3–0 nylon sutures. Postoperative antibiotics were given subcutaneously (gentamicin 0.5 mg/kg).

Seventeen preliminary trial operations were performed to confirm the reliability of this model. All operations were completed within 40 min. Deep infection occurred in one case, and two nonunions occurred. The overall fusion rate 42 days after surgery was 88%.

Experiment 1: quantitative reverse transcription and real-time polymerase chain reaction analysis

The mRNA expression level within the grafted bone was measured using reverse transcription-polymerase chain reaction (RT-PCR). Grafted bone was harvested on postoperative days 2, 4, 7, and 14 (Fig. 1C). The samples were frozen in liquid nitrogen and homogenized using a dismembrator. Total RNAs were extracted from the samples using standard TRIzol Reagent (Invitrogen Corp., Carlsbad, CA). For cDNA synthesis, 1 μg of RNA was reverse-transcribed using random hexamer primers (Promega, Madison, WI) and Improm-II reverse transcriptase (Promega). Real-time PCR was performed using OPTICON II (Bio-Rad Laboratories, Hercules, CA) in a 20-μl reaction volume. Signals were detected using the SYBR Green qPCR Kit (Finzymes, Espoo, Finland) with gene-specific primers designed using OLIGO (Molecular Biology Insights, Cascade, CO). Gene-specific primers of insulin-like growth factor 1 (IGF-1), bone morphogenetic protein-2, -4 and -7 (BMP-2, -4, and -7), alkaline phosphatase (ALP), osteocalcin (OC), osteonectin (ON), type I collagen (COL1A1), type II collagen (COL2A1), type X collagen (COL10A1), receptor activator of NFκB ligand (RANKL), osteoprotegerin (OPG), tartrate-resistant acid phosphatase (TRAP), calcitonin receptor (CTR), and glyceraldehyde 3-phosphate dehydrogenase (GAPDH) as a housekeeping gene are shown in Table 1. The relative mRNA expression of each targeted gene was normalized by the cycle threshold values of GAPDH.

Experiment 2: fusion and structural assessment

Fusion assessment

Fusion at the bone-grafted segment was assessed by manual palpation and soft X-ray observation at the L4–L5 segment. Immediately after death, the harvested lumbar spine was gently palpated, and lateral side-bending motion at the L4–L5 level was compared with the motion at the adjacent levels above (L3–L4) and below (L5–L6). Then, posteroanterior soft X-ray radiographs of the lumber spine were taken under consistent conditions (30 kV, 4 mA, for 150 s; SRO-M50D; Tanaka X-ray, MFG Co. Ltd., Tokyo, Japan). The formation of bridging bone between the L4 and L5 transverse processes and consolidation of the grafted bone was evaluated. According to the results of manual palpation testing and soft X-ray observation, the fusion status of each specimen was graded based on three categories. The specimen was graded as a solid union when no motion was observed; as an immature union when bony continuity between L4 and L5 transverse processes was observed but the segment had

Table 1
Gene-specific primers for RT-PCR

Gene	Accession no.	Sequence		Product length (bp)
		(Forward)	(Reverse)	
IGF-1	NM_178899	5′-CACCACAGACGGGCATIG-3	5′-TGCAGCGGACACAGTACATC-3	81
BMP-2	NM_017178	5′-TICCCCTGGCTGATCACC-3	5′-TGGAGATTGCGCTAAGCTCA-3	120
BMP-4	NM_012827	5′-GAACAGGGCTTCCACCGTAT-3	5′-GCAGGGCTCACATCGAAAG-3	146
BMP-7	XM_342591	5′-GAGCGGTTTGACAACGAGAC-3	5′-AGAAGCCCAGATGGTACGG-3	111
ALP	NM_013059	5′-GGGAGATGGTATGGGCGTCT-3	5′-CCCGTGTTGTGGTGTAGCTG-3	124
OC	M25490	5′-TCACAGGCTATGCGAGTTGG-3	5′-GGCTGGCCCTAGAGACGAG-3	114
ON	NM_012656	5′-TCGACTCTGAGGCCATAGC-3	5′-CTTATGCAATTCCCGTTTCC-3	92
COL1A1	XM_213440	5′-TTACTACCGGGCCGATGA-3	5′-CTGCGGATGTTCTCAATCTG-3	99
COL2A1	NM_012929	5′-CCCAACACCGCTAACGTC-3	5′-CTTCGTCCAGGTAGGCAATG-3	106
COL10A1	AJ131848	5′-CAGCCAAGCAGTCATACCTG-3	5′-TCACAGTAAAAGCGGACACC-3	122
RANKL	NM_057149	5′-TATGATGGAAGGTTCGTGGC-3	5′-ACTTTATGGGAACCCGATGG-3	92
OPG	NM_012870	5′-ACAGCTGGCACACGAGTGAT-3	5′-CCTTCCTCACATTCGCACAC-3	115
TRAP	NM_019144	5′-AGAACGGTGTGGGCTATGTG-3	5′-AAAGCGTAGGTAGCCGTTGG-3	95
CTR	NM_053816	5′-ATCATCCATGGACCCGTCAT-3	5′-CATGTAGGCCTCGGCTTCA-3	114
GAPDH	NM_017008	5′-GCTGGTCATCAACGGGAAA-3	5′-ACGCCAGTAGACTCCACGAC-3	143

slight motion; and as a nonunion when wide motion equivalent to adjacent segments was detected. Fusion rate was defined as the percentage of solid or immature union (Fig. 1D). The manual palpation testing used in this study is an approved alternative method to assess the stiffness of the fusion mass, because mechanical stiffness of the spinal segment is difficult to measure due to the small size of the grafted segment and the complicated shape of the rat spine [6,7,37].

Three-dimensional micro-computed tomography scanning and microstructural indices analysis of fusion mass

Three-dimensional (3D) micro-computed tomography scanning (μCT) in the axial plane was performed using a CT scanner (MCT-CB100MF; Hitachi Medical, Tokyo, Japan) to evaluate the calcified fusion mass at the intertransverse process region where bone did not originally exist. The scans were initiated from the lower endplate of the L4 vertebral body cranially in 13-μm sections, for a total of 135 slices per scan (Fig. 1D).

The cortical bone and trabecular bone were separated automatically, and microstructural indices were measured from the 3D reconstruction image using TRI/3D-BON (RATOC System Engineering, Tokyo, Japan). Bone volume/tissue volume (BV/TV), trabecular thickness (Tb.Th), trabecular number (Tb.N), and trabecular separation (Tb.Sp) were calculated using a parallel plate model. To analyze the 3D trabecular network structure, the number of nodes/trabecular sample volume (N.Nd/TV), the number of termini/trabecular sample volume (N.Tm/TV), and the number of connecting points with the cortical bone/trabecular sample volume (N.Ct/TV) were measured. In addition, a 3D reconstruction image of cortical bone was built, and average thickness of cortical bone (Ct) and cortical bone ratio (Cv/Av) were calculated.

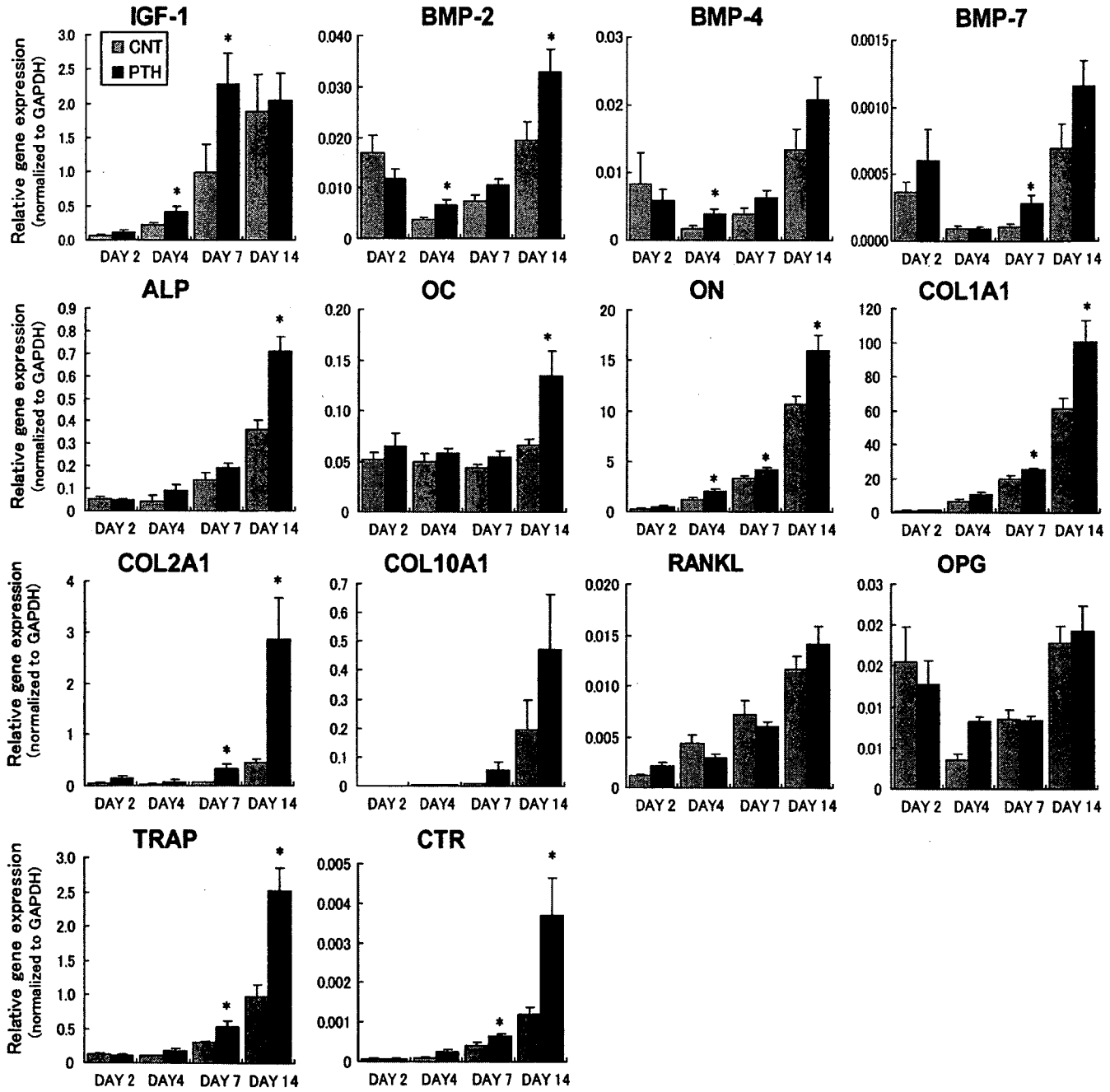

Fig. 2. mRNA expression level of targeted genes during first 14 days after surgery. The values of each target gene mRNA expression were normalized by the cycle threshold values of GAPDH. Data are expressed as mean±SEM. *$p<0.05$ vs. control group at each time point.

Histologic evaluation

The specimens were fixed with 70% ethanol. The undecalcified specimens were embedded in glycolmethacrylate, and sectioned at 3 μm in the axial plane. Sections were stained with toluidine blue O and observed under light and fluorescence microscopy. Histomorphometric analysis was performed to evaluate the fusion status and remodeling condition of the fusion mass. Mineral apposition rate (MAR) was calculated from the width of the double-labeled interval, and mineralized surface/bone surface (MS/BS) was calculated from the length of the bone surface and calcein-labeled surface. Osteoclast surface (Oc.S/BS) was calculated to evaluate bone resorption activity.

Serum bone metabolism markers

Blood samples were collected from the abdominal aorta before killing the rats and stored at −83 °C for analyzing serum bone metabolism markers. Osteocalcin and type I collagen crosslinked C-telopeptides (CTX) levels in the serum were assayed using an enzyme-lined immunosorbent assay kit (Nordic Bioscience Diagnostics A/S, Herlev, Denmark).

Statistical analysis

Differences in the fusion status between groups were analyzed with Chi-squared test. mRNA expression levels, microstructural indices, histomorphometry, and serum bone metabolism marker levels were expressed as mean±standard error of the mean. Differences between groups were determined by analysis of variance (ANOVA) followed by post hoc analysis with Fisher's protected least significant difference test. Results were considered significant at $p<0.05$.

Results

Experiment 1: mRNA expression of bone related genes at graft site

Time course changes in mRNA expression of osteoblast- and osteoclast-related genes during the first 14 days are shown in Fig. 2. In the control group, mRNA expression of osteoblast-related genes (*IGF-1*, *ALP*, *OC*, *ON*, *COL1A1*, *COL2A1*, and *COL10A1*), and osteoclast marker genes (*RANKL*, *TRAP* and *CTR*) gradually increased after the bone grafting procedure, whereas BMPs and OPG mRNA expression decreased from days 2 to 4 and increased from days 4 to 14. PTH treatment upregulated the mRNA expression levels of both osteoblast- and osteoclast-related genes, and there were significant differences in IGF-1 levels on days 4 and 7, BMP-2 on days 4 and 14, BMP-4 on day 4, BMP-7 on day 7, ALP on day 14, OC on day 14, ON on days 4, 7, and 14, COL1A1 on days 7 and 14, COL2A1 on days 7 and 14, TRAP on days 7 and 14, and CTR on days 7 and 14. PTH treatment did not affect RANKL and OPG mRNA expression.

Experiment 2: fusion assessment

Based on manual palpation testing, the L4–L5 spinal segment was stabilized at an earlier time point in the PTH group than in the control group. On day 14 after surgery, none of the specimens from either group were classified as a solid union; however, one of seven specimens in the control group and four of seven specimens in the PTH group were classified as immature unions. Fusion rate in the PTH group (57%) was higher than that in the control group (14%) on day 14 despite that there was no statistical difference in fusion rate between groups ($p=0.09$). On days 28 and 42, six of seven specimens in the control group and all seven specimens in the PTH group were classified as unions, and there was no significant difference in fusion rate between groups ($p=0.30$). Soft X-ray images showed that the bony bridging between the L4 and the L5 transverse processes was achieved in the successful fusion specimens and that PTH-treated animals had a larger and denser fusion mass compared to the vehicle-treated animals (Figs. 3B–G).

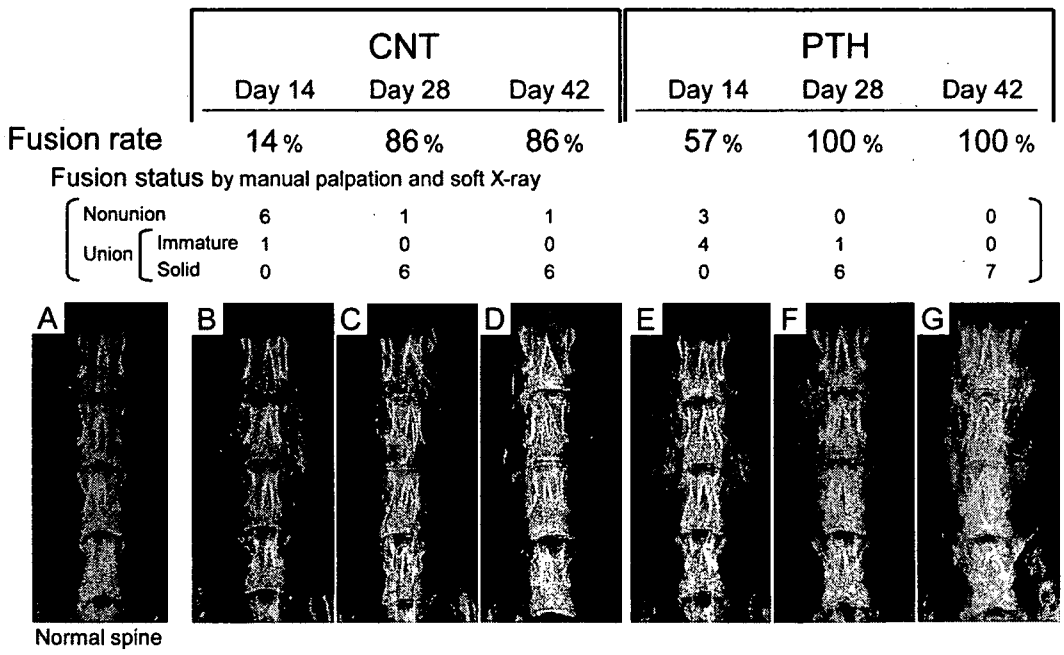

Fig. 3. The fusion assessment results. Fusion rate was calculated as the percentage of solid and immature unions. The results show that the fusion rate on day 14 was higher in the PTH group than in the control group. There was, however, no significant difference in the fusion rate between control and PTH groups on day 14 ($p=0.09$). Soft X-ray images of normal rat spine (A) and successful fusion specimens in both groups at each time point were shown (B–G). PTH group had a larger and denser fusion mass compared to the control group.

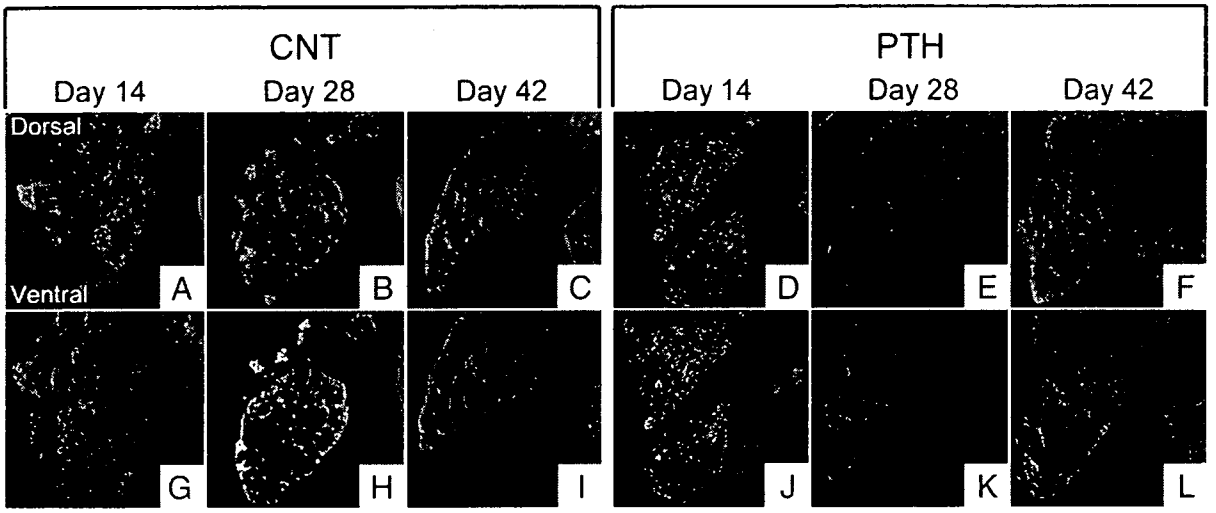

Fig. 4. Micro-computed tomography scanning of fusion mass: upper row (A–F) shows axial 2D images; lower row (G–L) shows reconstructed 3D images. On day 14, fusion mass mainly consisted of grafted bone fragments, while bone fragments were less visible and newly formed trabecular bone was observed in the PTH group (A and D). On day 28, grafted bone fragments were still visible in the control group, whereas they were not observed in the PTH group (B and E). On day 42, a structurally mature fusion mass consisting of a cortical shell surrounding the trabecular bone had formed in both group, and the cortical shell thickness was apparently higher in the PTH group compared to the control group (C and F).

3D micro-computed tomography images

On day 14, the fusion mass consisted of mainly dispersed grafted bone fragments and newly formed bone was observed in a limited area of the fusion mass in the control group (Figs. 4A and G), whereas the bone fragments were less visible and newly formed bone with a trabecular network was observed inside the fusion mass in the PTH group (Figs. 4D and J). On day 28, grafted bone fragments remained at the dorsal part of the fusion mass in the control group, but not in the PTH group (Figs. 4B and E). On day 42, the fusion masses in both groups developed a cortical shell around the trabecular bone, and the thickness of the cortical shell was greater in the PTH group compared to the control group (Figs. 4C and F).

Microstructural indices analysis

The trabecular volume and connectivity parameters of fusion mass (BV/TV, Tb.N, and N.Nd/TV) were significantly higher in the PTH group than in the control group at each time point throughout the observation period (Table 2). The trend of the time-related changes in these parameters, however, differed between groups: in the control group, BV/TV, Tb.N, and N.Nd/TV values increased from days 14 to 28, and decreased from days 28 to 42, whereas in the PTH group these values were highest on day 14 and decreased over time. On the other hand, Tb.Th, Ct, and Cv/Av gradually increased over time in both groups, except for the Ct value in the control group on day 14. An automatically calculated Ct value for the control group on day 14 is not available

Table 2
3D micro-CT microstructure indices analysis of the fusion mass

Group	CNT	PTH	CNT	PTH	CNT	PTH
	14 Days after surgery		28 Days after surgery		42 Days after surgery	
BV/TV (%)	19.1±1.9	47.8±3.3*	29.3±4.4	41.4±2.8*	25.4±1.7	34.4±1.3*
Tb.Th (μm)	41.3±2.0	50.2±3.4*	48.8±2.2	51.6±3.0	51.1±2.1	55.3±1.2*
Tb.N (l/mm)	4.6±0.3	9.7±1.2*	6.0±0.8	8.0±0.2*	5.0±0.3	6.2±0.2*
Tb.Sp (μm)	177.2±16.4	56.7±11.4*	129.4±28.7	73.9±5.3*	155.8±14.5	106.7±5.0*
Node strut						
N.Nd/TV (l/mm^3)	80.1±5.2	320.4±70.3*	127.3±24.1	188.9±10.3*	87.4±6.5	100.1±5.8
N.Tm/TV (l/mm^3)	59.7±17.1	31.6±10.5*	7.5±2.4	8.8±0.8	8.8±4.7	6.7±1.1
N.Ct/TV (l/mm^3)	177.1±9.3	447.36±149.7*	382.0±29.1	446.1±52.5	277.5±39.8	378.1±23.3
Ct (μm)	250.9±137.8	114.9±16.2	223.8±22.7	313.9±46.2*	299.2±81.3	395.2±30.1*
Cv/Av (%)	27.9±1.9	26.1±0.2	38.7±3.4	42.9±4.1	41.7±4.4	46.0±2.8

BV/TV, bone volume/tissue volume; Ct, average thickness of cortical bone; Cv/Av, cortical bone ratio; Tb.Th, trabecular thickness; Tb.N, trabecular number; Tb.Sp, trabecular separation; N.Nd/TV, number of mode/trabecular sample volume; N.Tm/TV, number of terminus/trabecular sample volume; N.Ct/TV, number of connecting pint with cortical bone/trabecular sample volume.
Data are expressed as means±SE.
* $p<0.05$ vs. CNT.

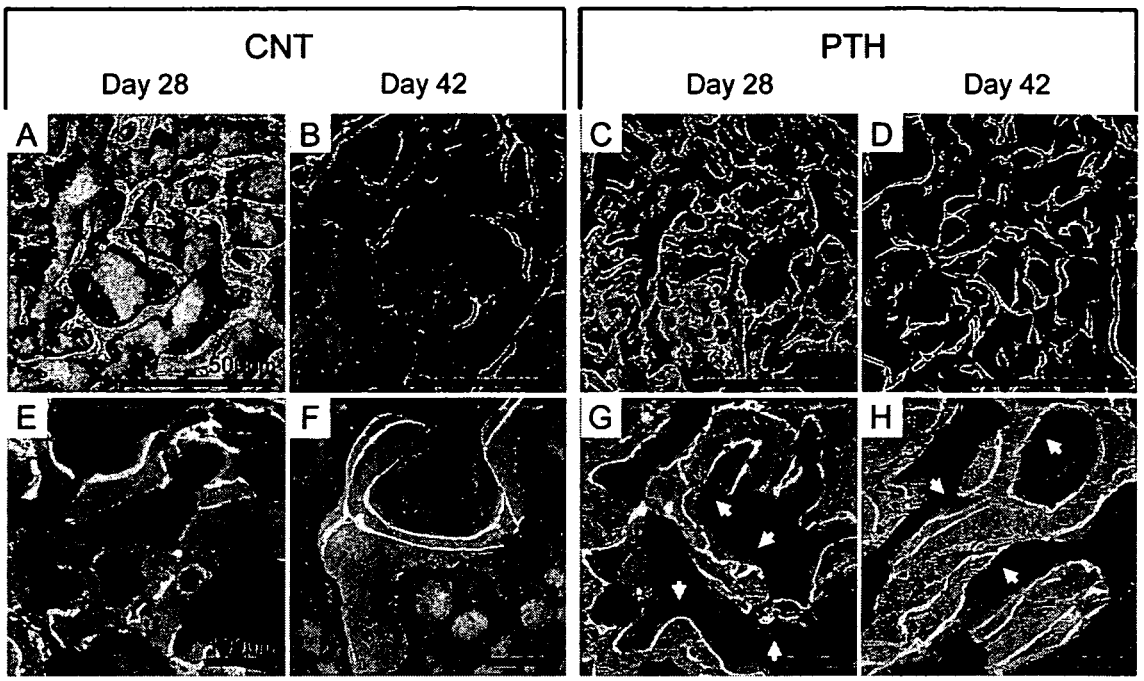

Fig. 5. Histologic features of the fusion mass: upper panels (A–D) show low magnification sections (×40) and lower panels (E–H) show high magnification sections (×200). The specimens in the PTH group had a larger calcein-labeled surface area compared to that in the control group. Active osteoblast cells (white arrows) were more frequently observed in the PTH-treated specimens on days 28 and 42 (G and H). (A–D: scale bars=500 μm) (E–H: scale bars=100 μm).

because the cortical shell was not yet formed in the control group on day 14. Tb.Th and Ct levels in the PTH group were significantly higher than those in the control group on day 42. Also, Tb.Th, Ct, and CV/AV in the PTH group on day 28 were equivalent to those in the control group on day 42.

Histologic evaluation

The PTH group had a larger calcein-labeled surface area on days 28 and 42 compared to the control group, and active osteoblast cells were frequently observed (Fig. 5). Bone histomorphometry indicated that the MAR and MS/BS values were significantly higher in the PTH group on both days 28 and 42. The Oc.S/BS values were also significantly higher in the PTH group on both days 28 and 42 (Table 3).

Table 3
Bone histomorphometry in fusion mass

	CNT	PTH
28 Days after surgery		
MAR (μm/day)	3.2±0.1	4.3±0.1**
MS/BS (%)	54.6±1.7	64.4±0.8*
Oc.S/BS (%)	7.1±1.2	11.3±1.2**
42 Days after surgery		
MAR (μm/day)	2.3±0.1	4.0±0.1**
MS/BS (%)	51.5±1.6	62.4±1.1**
Oc.S/BS (%)	4.7±0.6	6.8±1.6*

MAR, mineral apposition rate; MS/BS, mineralized surface/bone surface; Oc.S/BS, asteoclast surface/bone surface.
Data are expressed as means±SE.
* $p<0.05$.
** $p<0.01$.

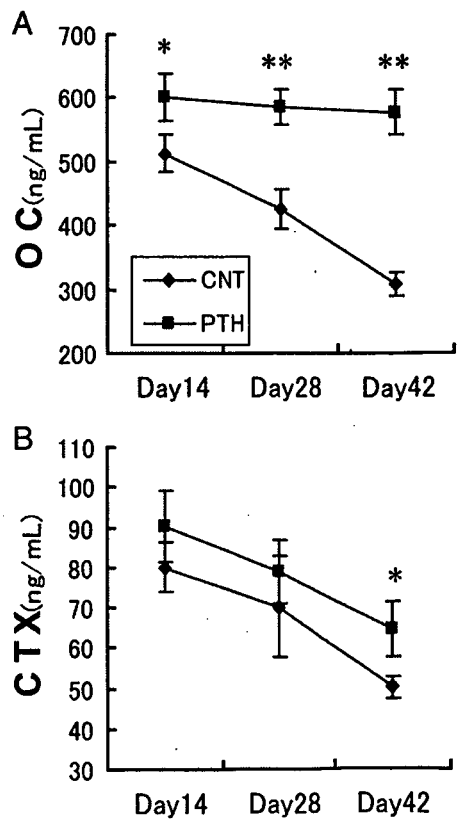

Fig. 6. Time course change in serum bone metabolism markers measured using an enzyme-lined immunosorbent assay. (A) Osteocalcin (OC); (B) type I collagen crosslinked C-telopeptides (CTX). Data are expressed as mean±SEM. *$p<0.05$. **$p<0.01$.

Serum bone metabolism markers

Serum OC levels were significantly higher in the PTH group than in the control group throughout the observation period. The serum OC level in the control group gradually decreased from days 14 to 42, whereas the serum OC levels in the PTH group remained the same from days 14 to 42 (Fig. 6A). Serum CTX levels tended to decrease gradually over time in both groups. The CTX levels in the PTH group were higher than in the control group at each time point, but were significantly different only on day 42 (Fig. 6B).

Discussion

PTH has a unique mechanism of action on bone: continuous administration of PTH leads to a decrease in bone volume (catabolic effect) [18,28,35], and intermittent administration of PTH leads to the formation of increased amounts of trabecular bone (anabolic effect) [12,13,26]. Although the mechanisms whereby intermittent PTH enhances bone formation are complicated and not well understood, the efficacy and safety of systemic PTH therapy as a bone-forming agent have been approved for the treatment of severe osteoporosis in men and women. This anabolic effect of PTH also provides a rationale for its potential use in the treatment of other skeletal disorders. Indeed, recent studies demonstrated that PTH treatment enhances fracture healing and the consolidation of distraction osteogenesis [38]. Especially in the fracture healing process, intermittent treatment with PTH increases union rate, amount of callus, bone mineral density, and mechanical strength [1–3,19,24,32]. The results of these studies suggest that the anabolic effect of PTH is more dramatic in newly forming bone than in bone that is undergoing normal remodeling [38,39]. In this study using a rat spinal arthrodesis model, we provide evidence that PTH(1–34) accelerates and enhances the healing process of bone grafts.

Our observations using 3D micro-CT clearly showed an enhancing effect of PTH on bone modeling and remodeling in the healing process of bone grafts, as illustrated in Fig. 7. From a histomorphometric point of view, we characterized the positive effects of intermittent administration of PTH(1–34) by three different measures: (1) grafted bone resorption; (2) cancellous bone modeling and remodeling; and (3) cortical shell formation.

Fresh autografts provide viable stem cells and osteoblasts that might "jump-start" new bone formation, and also contain several osteoinductive factors that stimulate osteogenic cell proliferation and differentiation. Graft bone resorption, however, is essential for subsequent new bone formation and remodeling in bone graft healing [11,17,41,47]. In this study, we showed that intermittent PTH treatment accelerated graft bone resorption in the early phase of healing. Micro-CT observation indicated that the graft bone fragment was resorbed and replaced with newly formed bone up to day 28 in PTH-treated animals, whereas it was still visible on day 28 in control animals. It is possible that this phenomenon derived from the PTH-stimulated enhancement of bone resorbing activity. Increased expression of both TRAP and CTR as osteoclast marker genes, the higher serum CTX levels, and the higher Oc.S/BS values in PTH-treated animals support this idea.

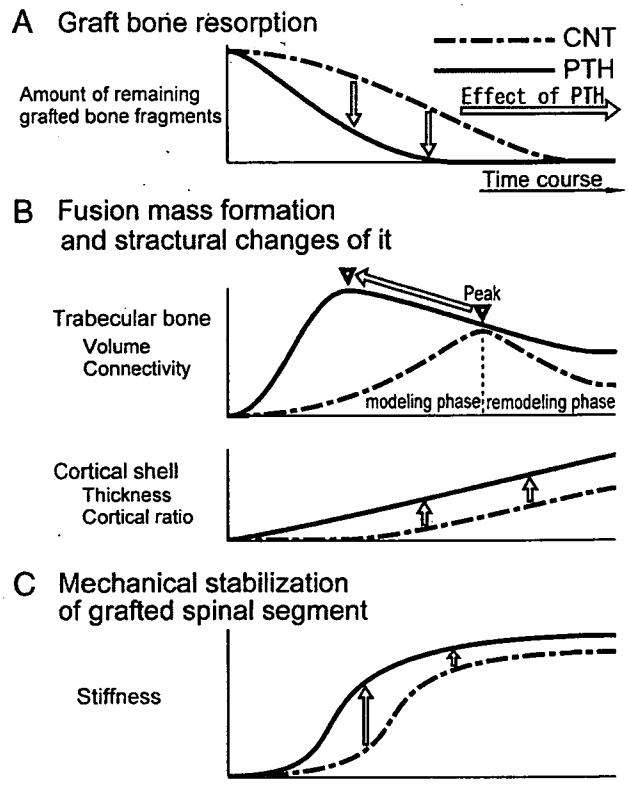

Fig. 7. Hypothetical model of the healing process of bone graft and the effect of intermittent PTH treatment on bone graft healing. (A) Graft bone resorption. PTH treatment accelerates graft bone resorption. (B) Calcified fusion mass formation and microstructural changes of the fusion mass. From the point of view of the changes in the structural characteristics of trabecular bone, initially formed "fine" trabecular bone is replaced by "thick and coarse" trabecular bone. The initial increase in trabecular bone volume and connectivity (BV/TV, Tb.N, and N.Nd/TV) is relevant to the modeling of fine trabecular bone, and the subsequent decrease in the levels of these markers is relevant to the remodeling of trabecular bone to the thick and coarse form. PTH treatment accelerates and enhances these modeling and remodeling process of the fusion mass. As to the cortical shell formation, PTH treatment increases cortical thickness (Ct) and cortical ratio (Cv/AV). (C) Mechanical stabilization of the grafted spinal segment. PTH treatment accelerates the stabilization process of the bone-grafted spinal segment.

The catabolic effect of PTH, which is mediated by RANKL and OPG, is induced by continuous administration of PTH, but not by intermittent administration of PTH in vitro [15,27,28,35]. In vivo and clinical studies, however, demonstrated that intermittent PTH treatment also upregulates bone resorbing activity concurrently with bone formative activity [4,9,32]. Buxton reported that intermittent PTH treatment enhances osteoclastogenesis by increasing RANKL and decreasing OPG in osteoporosis patients treated with intermittent administration of PTH [9]. Although we could not detect a significant difference in RANKL and OPG mRNA expression between PTH-treated and vehicle-treated animals, we speculate that intermittent PTH treatment might affect osteoclast maturation and function by regulating the RANKL and OPG expression in the osteoblast lineage cells.

PTH-treated animals attained a fusion mass with a larger and denser trabecular volume at an earlier time point compared to vehicle-treated animals. In the bone graft healing process in normal rat, trabecular volume reaches a peak at day 28, and

thereafter gradually declines in a similar manner to that which is observed during fracture callus remodeling [17]. The same tendency was observed in PTH-treated animals; however, the trabecular volume peaked at day 14. Furthermore, the trabecular volume in PTH-treated animals was greater than that in vehicle-treated animals throughout the observation period. These findings indicate that PTH(1–34) decreased the modeling and remodeling period as well as generated a larger area of trabecular bone in the bone graft surgery. Initially formed "fine" trabecular bone is replaced by "thick and coarse" trabecular bone in response to mechanical stress [17,47]. PTH also enhanced and accelerated the structural maturation of trabecular bone.

Cortical shell formation of the fusion mass was faster and thicker in PTH-treated animals at each time point throughout the observation period. New cortical shell formation appeared on day 14 in PTH-treated animals, whereas the cortical shell first appeared on day 28 in most vehicle-treated animals. This is a striking observation because the cortical shell is thought to be the most important determinant for the mechanical strength of bone. Indeed, the mechanical strength of regenerated bone correlates with cortical shell thickness in a PTH-treated fracture model [24]. This finding suggests that systemic PTH treatment enhances mechanical strength of the fusion mass, despite the lack of data regarding the mechanical strength of the fusion mass in our spinal arthrodesis model. Although it does not directly represent the mechanical strength of the fusion mass, manual palpation testing indicated that PTH-treated animals obtained earlier stabilization of the grafted spinal segment compared to the vehicle-treated animals. These results suggest that PTH enhances the stabilization of bone-grafted spinal arthrodesis segments by generating a thicker cortical shell in a shorter time period as well as by generating denser and larger cancellous bone.

These anabolic effects of intermittent PTH administration on graft bone healing must derive from the predominant effect of PTH on bone formation. Increased mRNA expression of osteoblastic bone matrix proteins, higher MAR and MS/BS values, and consistently higher serum OC levels as systemic bone formation markers in the PTH group support this idea. Previous in vivo studies demonstrated that the anabolic effects of PTH on bone formation are mediated by IGF-1, which stimulates proliferation and differentiation of osteoblasts and increases collagen synthesis [30,32,45]. The earlier increase in IGF-I mRNA expression in the PTH group, which precedes ALP and bone matrix protein mRNA expression in our study, might support this idea. We also found the elevated levels of BMPs mRNA expression in PTH-treated animals after 4 postoperative days despite that there has been no direct in vitro evidence that PTH alters BMPs gene expression. Our data, however, showed the possibility that intermittent administration of PTH enhanced BMPs genes expression directly or indirectly in the healing process of bone graft. There is no doubt that osteoblasts, their precursors, and the marrow stromal cells have central roles in the bone formation actions of PTH; however, PTH might also enhance chondrocyte proliferation and differentiation, which are essential for subsequent endochondral bone formation.

Interestingly, there was a delay in the increase in bone-related gene expression compared to a previously reported rat fracture healing model. The expression peaks of IGF-1 mRNA (days 7–14), bone matrix proteins (day 14), and osteoclast-related genes (day 14) in the control animals in the present study were delayed compared with those in previously reported rat femur fracture models (IGF-1, days 4–7; ALP and other bone matrix proteins, day 7; osteoclast-related gene and TRAP index, day 7) [25,32]. This delay suggests that graft bone healing differs from fracture healing [17]. In the long bone fracture healing process, mesenchymal stem cells, which proliferate and differentiate into osteoprogenitor cells, are easily recruited from the bone marrow and periosteum, then differentiate into osteoblasts and rapidly synthesize bone matrix. In contrast, more time is required to achieve graft bone revascularization, which is essential for promoting osteoprogenitor cell differentiation [47]. Therefore, intermittent PTH treatment might be more effective for adjuvant chemotherapy in bone graft surgery compared to fracture treatment.

There are some limitations to this study. Rats are four-footed rodents. The mechanical environment at the grafted spinal segment and the healing process of grafted bone are different from those in humans. Therefore, the results of the present study are not completely applicable to graft bone healing in human spinal arthrodesis surgery. We think it necessary to perform further experimental animal studies using higher species such as primates before human clinical trials. Previous reports, however, indicate that the anabolic effects of PTH observed in animal models also occur in clinical studies of osteoporosis [10,12,13,20,26,33], so it is estimated that intermittent administration of PTH might advantageously affect graft bone surgery. In the present study, we did not assess mechanical strength of the fusion segment. Because the rat spine is very small and has a complicated shape, it is impossible to accurately measure the mechanical strength of the rat grafted spinal segment. The goal of spinal arthrodesis surgery, however, is to stabilize the grafted spinal segment. The results of the present study demonstrated that early stabilization of the fused spinal segment based on manual palpation testing was achieved by intermittent administration of PTH(1–34), and also that the maturation of microstructural properties of the fusion mass, which positively correlates with mechanical strength [22,23,40], was accelerated and enhanced by PTH administration.

We conclude that intermittent administration of human PTH (1–34) decreased the period of time required for graft bone healing and produced a more solid fusion mass in the rat posterolateral spinal arthrodesis model. Because the time until full recovery is up to 6 months after spinal fusion surgery, the accelerating effect of PTH on bone graft healing might be beneficial for spinal fusion surgery and other skeletal diseases requiring bone grafts. Furthermore, in contrast to the need for long-term administration of PTH for the treatment of osteoporosis, a few months of short-term administration should be sufficient to obtain solid fusion in spinal arthrodesis surgery. Short-term administration might not increase the risk for osteosarcoma, which may be induced by the long-term administration of high-dose PTH [42].

Thus, we expect that intermittent administration of PTH(1–34) might be an efficient adjuvant intervention for spinal arthrodesis surgery and all other orthopedic surgeries requiring bone grafts.

Acknowledgments

The authors thank Asahi Kasei Co. for supplying the hPTH (1–34) and for participating in imaging study. Manufacturer names: Asahi Kasei Co., Ltd. (Tokyo, Japan); Bio-Rad Laboratories, Hercules, CA; Finnzymes Oy, Finland; Invitrogen, Carlsbad, CA; MJ Research, Hercules, CA; Molecular Biology Insights, Cascade, CO; Nordic Bioscience Diagnostics A/S, Herlev, Denmark; Promega, Madison, WI; Qiagen, Hilden, Germany; Sigma Chemical Co., St. Louis, MO; Wako Ltd., Osaka, Japan.

References

[1] Alkhiary YM, Gerstenfeld LC, Krall E, Westmore M, Sato M, Mitlak BH, et al. Enhancement of experimental fracture-healing by systemic administration of recombinant human parathyroid hormone (PTH 1–34). J Bone Joint Surg Am 2005;87:731–41.

[2] Andreassen TT, Ejersted C, Oxlund H. Intermittent parathyroid hormone (1–34) treatment increases callus formation and mechanical strength of healing rat fractures. J Bone Miner Res 1999;14:960–8.

[3] Andreassen TT, Willick GE, Morley P, Whitfield JF. Treatment with parathyroid hormone hPTH(1–34), hPTH(1–31), and monocyclic hPTH (1–31) enhances fracture strength and callus amount after withdrawal fracture strength and callus mechanical quality continue to increase. Calcif Tissue Int 2004;74:351–6.

[4] Black DM, Bilezikian JP, Ensrud KE, Greenspan SL, Palermo L, Hue T, et al. One year of alendronate after one year of parathyroid hormone (1–84) for osteoporosis. N Engl J Med 2005;353:555–65.

[5] Boden SD. Overview of the biology of lumbar spine fusion and principles for selecting a bone graft substitute. Spine 2002;27:S26–31.

[6] Boden SD, Schimandle JH, Hutton WC. An experimental lumbar intertransverse process spinal fusion model. Radiographic, histologic, and biomechanical healing characteristics. Spine 1995;20:412–20.

[7] Boden SD, Titus L, Hair G, Liu Y, Viggeswarapu M, Nanes M, et al. Lumbar spine fusion by local gene therapy with a cDNA encoding a novel osteoinductive protein (LMP-1). Spine 1998;23:2486–92.

[8] Bridwell KH, Sedgewick TA, O'Brien MF, Lenke LG, Baldus C. The role of fusion and instrumentation in the treatment of degenerative spondylolisthesis with spinal stenosis. J Spinal Disord 1993;6:461–72.

[9] Buxton EC, Yao W, Lane NE. Changes in serum receptor activator of nuclear factor-kappaB ligand, osteoprotegerin, and interleukin-6 levels in patients with glucocorticoid-induced osteoporosis treated with human parathyroid hormone (1–34). J Clin Endocrinol Metab 2004;89:3332–6.

[10] Cosman F, Nieves J, Woelfert L, Formica C, Gordon S, Shen V, et al. Parathyroid hormone added to established hormone therapy: effects on vertebral fracture and maintenance of bone mass after parathyroid hormone withdrawal. J Bone Miner Res 2001;16:925–31.

[11] Cypher TJ, Grossman JP. Biological principles of bone graft healing. J Foot Ankle Surg 1996;35:413–7.

[12] Dempster DW, Cosman F, Kurland ES, Zhou H, Nieves J, Woelfert L, et al. Effects of daily treatment with parathyroid hormone on bone microarchitecture and turnover in patients with osteoporosis: a paired biopsy study. J Bone Miner Res 2001;16:1846–53.

[13] Dempster DW, Cosman F, Parisien M, Shen V, Lindsay R. Anabolic actions of parathyroid hormone on bone. Endocr Rev 1993;14:690–709.

[14] DeWald C, Stanley J. Instrumentation-related complications of multilevel fusions for adult spinal deformity patients over age 65: surgical considerations and treatment options in patients with poor bone quality. Spine 2006;31:S144–51.

[15] Ferrari SL, Pierroz DD, Glatt V, Goddard DS, Bianchi EN, Lin FT, et al. Bone response to intermittent parathyroid hormone is altered in mice null for {beta}-Arrestin2. Endocrinology 2005;146:1854–62.

[16] Finkelstein JS, Klibanski A, Schaefer EH, Hornstein MD, Schiff I, Neer RM. Parathyroid hormone for the prevention of bone loss induced by estrogen deficiency. N Engl J Med 1994;331:1618–23.

[17] Hing KA. Bone repair in the twenty-first century: biology, chemistry or engineering? Philos Transact A Math Phys Eng Sci 2004;362:2821–50.

[18] Hock JM, Gera I. Effects of continuous and intermittent administration and inhibition of resorption on the anabolic response of bone to parathyroid hormone. J Bone Miner Res 1992;7:65–72.

[19] Holzer G, Majeska RJ, Lundy MW, Hartke JR, Einhorn TA. Parathyroid hormone enhances fracture healing. A preliminary report. Clin Orthop Relat Res 1999:258–63.

[20] Horwitz MJ, Tedesco MB, Gundberg C, Garcia-Ocana A, Stewart AF. Short-term, high-dose parathyroid hormone-related protein as a skeletal anabolic agent for the treatment of postmenopausal osteoporosis. J Clin Endocrinol Metab 2003;88:569–75.

[21] Huang RC, Khan SN, Sandhu HS, Metzl JA, Cammisa FP, Zheng F, et al. Alendronate inhibits spine fusion in a rat model. Spine 2005;30:2516–22.

[22] Ito M, Nishida A, Koga A, Ikeda S, Shiraishi A, Uetani M, et al. Contribution of trabecular and cortical components to the mechanical properties of bone and their regulating parameters. Bone 2002;31:351–8.

[23] Kinney JH, Ladd AJ. The relationship between three-dimensional connectivity and the elastic properties of trabecular bone. J Bone Miner Res 1998;13:839–45.

[24] Komatsubara S, Mori S, Mashiba T, Nonaka K, Seki A, Akiyama T, et al. Human parathyroid hormone (1–34) accelerates the fracture healing process of woven to lamellar bone replacement and new cortical shell formation in rat femora. Bone 2005;36:678–87.

[25] Kon T, Cho TJ, Aizawa T, Yamazaki M, Nooh N, Graves D, et al. Expression of osteoprotegerin, receptor activator of NF-kappaB ligand (osteoprotegerin ligand) and related proinflammatory cytokines during fracture healing. J Bone Miner Res 2001;16:1004–14.

[26] Lindsay R, Nieves J, Formica C, Henneman E, Woelfert L, Shen V, et al. Randomised controlled study of effect of parathyroid hormone on vertebral-bone mass and fracture incidence among postmenopausal women on oestrogen with osteoporosis. Lancet 1997;350:550–5.

[27] Locklin RM, Khosla S, Turner RT, Riggs BL. Mediators of the biphasic responses of bone to intermittent and continuously administered parathyroid hormone. J Cell Biochem 2003;89:180–90.

[28] Ma YL, Cain RL, Halladay DL, Yang X, Zeng Q, Miles R, et al. Catabolic effects of continuous human PTH (1–38) in vivo is associated with sustained stimulation of RANKL and inhibition of osteoprotegerin and gene-associated bone formation. Endocrinology 2001;142:4047–54.

[29] McGuire RA, Amundson GM. The use of primary internal fixation in spondylolisthesis. Spine 1993;18:1662–72.

[30] Miyakoshi N, Kasukawa Y, Linkhart TA, Baylink DJ, Mohan S. Evidence that anabolic effects of PTH on bone require IGF-I in growing mice. Endocrinology 2001;142:4349–56.

[31] Mofidi A, Sedhom M, O'Shea K, Fogarty EE, Dowling F. Is high level of disability an indication for spinal fusion? Analysis of long-term outcome after posterior lumbar interbody fusion using carbon fiber cages. J Spinal Disord Tech 2005;18:479–84.

[32] Nakajima A, Shimoji N, Shiomi K, Shimizu S, Moriya H, Einhorn TA, Yamazaki M. Mechanisms for the enhancement of fracture healing in rats treated with intermittent low-dose human parathyroid hormone (1–34). J Bone Miner Res 2002;17:2038–47.

[33] Neer RM, Arnaud CD, Zanchetta JR, Prince R, Gaich GA, Reginster JY, et al. Effect of parathyroid hormone (1–34) on fractures and bone mineral density in postmenopausal women with osteoporosis. N Engl J Med 2001;344:1434–41.

[34] Ondra SL, Marzouk S. Revision strategies for lumbar pseudarthrosis. Neurosurg Focus 2003;15:E9.

[35] Qin L, Raggatt LJ, Partridge NC. Parathyroid hormone: a double-edged sword for bone metabolism. Trends Endocrinol Metab 2004;15:60–5.

[36] Salamon ML, Althausen PL, Gupta MC, Laubach J. The effects of BMP-7 in a rat posterolateral intertransverse process fusion model. J Spinal Disord Tech 2003;16:90–5.

[37] Schimandle JH, Boden SD. Spine update. The use of animal models to study spinal fusion. Spine 1994;19:1998–2006.

[38] Seebach C, Skripitz R, Andreassen TT, Aspenberg P. Intermittent parathyroid hormone (1–34) enhances mechanical strength and density of new bone after distraction osteogenesis in rats. J Orthop Res 2004;22:472–8.

[39] Skripitz R, Andreassen TT, Aspenberg P. Strong effect of PTH (1–34) on regenerating bone: a time-sequence study in rats. Acta Orthop Scand 2000;71:619–24.
[40] Ulrich D, van Rietbergen B, Laib A, Ruegsegger P. The ability of three-dimensional structural indices to reflect mechanical aspects of trabecular bone. Bone 1999;25:5–60.
[41] Vaccaro AR, Chiba K, Heller JG, Patel T, Thalgott JS, Truumees E, et al. Bone grafting alternatives in spinal surgery. Spine J 2002;2:206–15.
[42] Vahle JL, Sato M, Long GG, Young JK, Francis PC, Engelhardt JA, et al. Skeletal changes in rats given daily subcutaneous injections of recombinant human parathyroid hormone (1–34) for 2 years and relevance to human safety. Toxicol Pathol 2002;30:312–21.
[43] West III JL, Bradford DS, Ogilvie JW. Results of spinal arthrodesis with pedicle screw-plate fixation. J Bone Joint Surg Am 1991;73:1179–84.
[44] Whitecloud III TS, Davis JM, Olive PM. Operative treatment of the degenerated segment adjacent to a lumbar fusion. Spine 1994;19:531–6.
[45] Yamaguchi M, Ogata N, Shinoda Y, Akune T, Kamekura S, Terauchi Y, et al. Insulin receptor substrate-1 is required for bone anabolic function of parathyroid hormone in mice. Endocrinology 2005;146:2620–8.
[46] Zdeblick TA. A prospective, randomized study of lumbar fusion. Preliminary results. Spine 1993;18:983–91.
[47] Zipfel GJ, Guiot BH, Fessler RG. Bone grafting. Neurosurg Focus 2003;14:e8.

Eur Spine J (2007) 16:2215–2224
DOI 10.1007/s00586-007-0501-0

ORIGINAL ARTICLE

Effect of Hydroxyapatite porous characteristics on healing outcomes in rabbit posterolateral spinal fusion model

Makoto Motomiya · Manabu Ito · Masahiko Takahata · Ken Kadoya · Kazuharu Irie · Kuniyoshi Abumi · Akio Minami

Received: 7 February 2007 / Revised: 30 June 2007 / Accepted: 3 September 2007 / Published online: 22 September 2007

Abstract Hydroxyapatite (HA) has been commonly used as a bone graft substitute in various kinds of clinical fields. To improve the healing capability of HA, many studies have been performed to reveal its optimal structural characteristics for better healing outcomes. In spinal reconstruction surgery, non-interconnected porous HAs have already been applied as a bone graft extender in order to avoid autogenous bone harvesting. However, there have been few experimental studies regarding the effects of the structural characteristics of HA in posterolateral lumbar intertransverse process spine fusion (PLF). The aims of this study were to investigate the effect of HA porous characteristics on healing outcomes in a rabbit PLF model in order to elucidate appropriate structural characteristics of HA as a bone graft extender. Thirty-six adult female Japanese White rabbits underwent bilateral intertransverse process fusion at the level of L5–6 without internal fixation. We prepared three types of HA with different porosities: HA with 15% porosity (HA15%), HA with 50% porosity (HA50%), and HA with 85% porosity (HA85%), all of which were clinically available materials. The HA15% and HA50% had few interconnecting pores, whereas the HA85%, which was a recently developed material, had abundant interconnecting pores. All rabbits were randomly divided into the following four groups according to the grafted materials: (1) HA15% + autogenous bone, (2) HA50% + autogenous bone, (3) HA85% + autogenous bone, (4) pure autogenous bone graft. The animals were euthanized at 5 weeks after surgery, and post-mortem analyses including biomechanical testing, radiographical and histological evaluations were performed. There was no statistically significant difference in either fusion rate and/or bending stiffness among the three HA groups. However, in histological and radiological analyses, both bone ingrowth rate and direct bone bonding rate in the HA85% group were significantly higher than those in the HA15% and HA50% groups, despite the similar value of bone volume rate in fusion mass among the three HA groups. In the HA85% group, bone ingrowth was achieved throughout the implanted HAs via interconnecting pores and there was excellent unification between the HA granules and the newly mineralized bone. On the other hand, in the non-interconnected porous HA groups, only a little bone ingrowth could be seen at the peripheral pores of the implanted HA, and its surface was mostly covered with fibrous tissue or empty space. The current study demonstrated that the HA porous characteristics had an effect on the histological outcomes in a rabbit PLF model. We would like to conclude that the interconnected high porous structure seems to be promising for the environment of PLF in the point of producing fusion mass with higher cellular viability. This is because the HA85% is superior in terms of integration with the newly formed bone in fusion mass compared to the non-interconnected porous HAs. However, the porous modifications of HA have little influence on fusion rate and mechanical strength because primary stabilization of the fusion segment is mainly achieved by bridging bone between the adjacent transverse processes outside the implanted materials, rather than the

M. Motomiya · M. Ito (✉) · M. Takahata · K. Kadoya · K. Abumi · A. Minami
Department of Orthopaedic Surgery,
Hokkaido University Graduate School of Medicine,
Kita-15 Nishi-7, Kita-ku, Sapporo 060-8638, Japan
e-mail: maito@med.hokudai.ac.jp

K. Irie
Department of Oral Anatomy, Health Sciences
University of Hokkaido School of Dentistry,
Ishikari-Tobetsu, Japan

degree of integration between the newly formed bone and the HA granules in PLF.

Keywords Bone graft substitute · Hydroxyapatite · Spine fusion · Porous characteristics · Interconnecting pore

Introduction

Bone graft surgeries have been widely performed in various fields such as orthopaedic, craniomaxillofacial, dental, and plastic surgery. Autogenous bone has been commonly used for bone graft surgery as the gold standard material. However, there have been a lot of morbidities associated with the harvest of autogenous bone such as long-lasting pain, deep infection, vascular injuries, and blood loss at the donor site [28, 33]. The limited volume of autogenous bone is also a disadvantage, especially in the case of patients with osteoporosis or with multiple previous bone graft procedures [3, 4, 27]. Therefore many researchers have developed and studied various kinds of bone graft substitutes in order to avoid bone graft harvesting.

Of all bone graft substitutes, Hydroxyapatite (HA) is one of the most popular materials and has been utilized experimentally and clinically in bone graft surgery because HA is a biocompatible material with excellent osteoconductivity [10, 20, 21]. However, clinical outcomes of the conventional HAs have not been superior to that of autogenous bone graft. In order to improve the healing capability of HA in bone graft surgery, many studies have been performed to reveal its optimal structural characteristics for bone healing [8, 9, 18, 19]. For example, for the non-weight bearing applications such as metaphyseal bone defects, the optimal porous structure of HA is believed to be the interconnected high porous structure with suitable pore size of approximately 300 μm [8, 9]. Tamai et al. [29] reported that abundant interconnected space promotes infiltration of bone tissue, bone marrow, and blood vessels, and allows bone remodeling throughout the material. On the other hand, for the weight-bearing applications such as spinal interbody fusion, a dense HA with adequate mechanical strength is beneficial to support the operated segment [16, 32]. Although high porous structure of HA is also preferable for spinal interbody fusion in terms of its superior integration with host bone tissue, this structure of HA cannot withstand severe cyclic mechanical loading. In this way, it is important to choose the proper structural characteristics of HA according to grafted environments.

Posterolateral lumbar intertransverse process spine fusion (PLF) is a commonly performed bone graft surgeries [4]. In PLF, the conventional non-interconnected porous HA has already been applied as bone graft extenders [4, 27, 30]. However, most surgeons are using it without consideration of the effects of its porous characteristics on healing outcomes in PLF. As many researchers reported, the grafted environment of PLF is significantly different from those of other operations such as metaphyseal bone defect and spinal interbody fusion in the following two points [4, 5, 27]. The first is that grafted materials in the environment of PLF are exposed to excessive distraction or tension loads, which may cause non-union of the fusion segment. Second is that the grafted materials are surrounded by less osteogenic environments such as muscle and other soft tissues, not bone tissue. Despite the above-mentioned unique environment of the grafted site, to our knowledge there has been little information about optimal porosity and geometrical porous design of HA as a bone graft extender in PLF.

The purpose of this study was to investigate the effect of HA porous characteristics on healing outcomes in a rabbit PLF model in order to elucidate appropriate structural characteristics of HA as a bone graft extender.

Materials and methods

Material preparation

We prepared three types of HA with different porosities (15, 50, and 85%) for this PLF experiment. The HAs with 15% porosity (HA15%) and with 50% porosity (HA50%) (APACERAM, PENTAX Corp., Tokyo, Japan) are conventionally available materials. Whereas the HA with 85% porosity (HA85%) (APACERAM-AX, PENTAX Corp., Tokyo, Japan), the highest among the clinically available HAs, has recently been developed using a new technique [26].

The structural characteristics of each HA under a scanning electron microscope (SEM) are shown in Fig. 1. As shown in Fig. 1a, d, the HA15% had a mostly dense body with scattered small-sized macropores. Figure 1b, e showed that the HA50% had many solitary large-sized macropores. There were few porous interconnections between each macropore in the HA15% and HA50%. On the other hand, SEM photographs of the HA85% showed that the material had a cancellous bone-like structure with abundant interconnecting pores and a microporous surface in every macropore (Fig. 1c, f). The detailed porous characteristics of each HA are listed in Table 1. As shown in Table 1, initial compressive strength gradually decreases in correlation with increasing porosity.

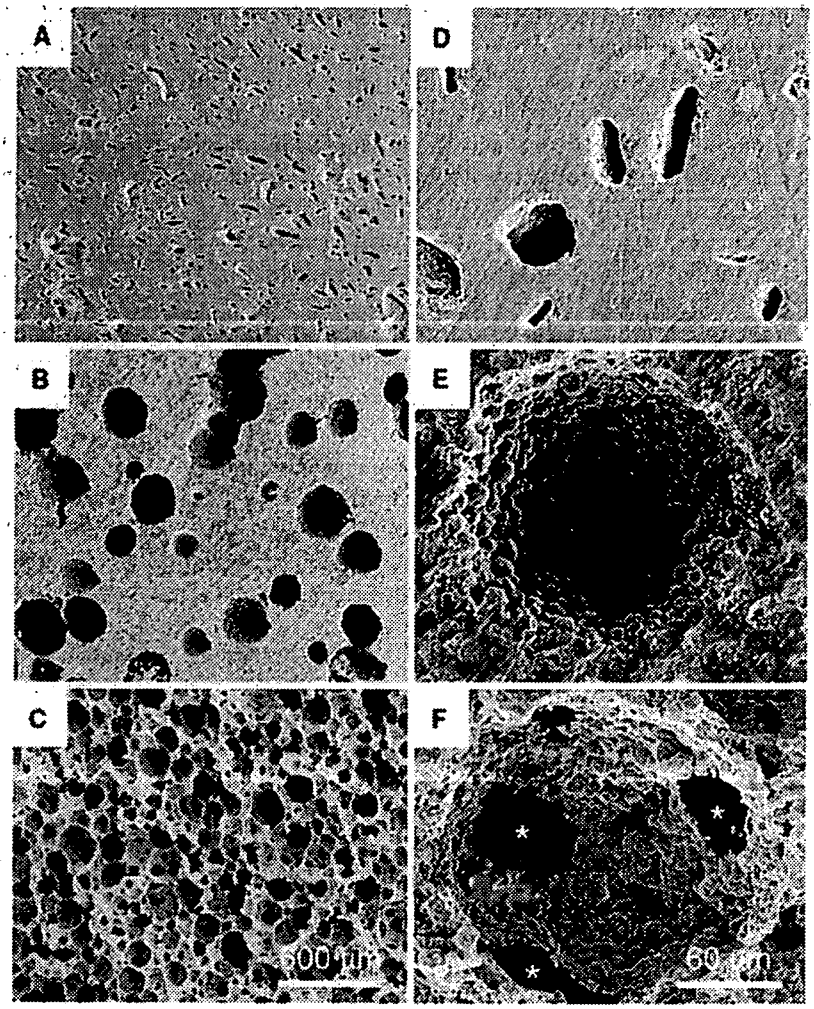

Fig. 1 Scanning electron microscopic appearance of the HA surface. **a**, **d** The HA15% has a mostly dense body with scattered small-sized macropores. **b**, **e** The HA50% has many solitary large-sized macropores. Each macropore has microporous surface and few porous interconnections. **c**, **f** The HA85% has a cancellous bone-like structure with abundant interconnecting pores (*asterisk*) about 50 μm in diameter and a microporous surface in every macropore

Table 1 The porous characteristics of HA

	Porosity (%)	Interconnecting pores	Pore size (μm)	Initial strength (MPa)
HA15%	15	–	10–50	240
HA50%	50	–	50–500	30
HA85%	85	+ (Average 90 μm)	50–300	2

Experimental posterolateral spine fusion in a rabbit model

The experimental protocol of this animal study was reviewed and approved by the Institutional Animal Care and Use Committee. Thirty-six adult female Japanese White rabbits (2.9–3.4 kg) were obtained from CLEA Japan, Inc. and were divided into the following four groups according to the grafted materials:

(1) HA15% + autogenous bone (n = 11)
(2) HA50% + autogenous bone (n = 9)
(3) HA85% + autogenous bone (n = 10)
(4) Pure autogenous bone graft (Auto) (n = 6)

Operative procedure

All rabbits underwent bilateral intertransverse process arthrodesis at the level of L5–6 without internal fixation [7]. General anesthesia was induced with an intravenous administration of sodium pentobarbital (20 mg/kg) and maintained with 2% isoflurane. Just before surgery Benzylpenicillin Potassium (Penicillin G Potassium, Meiji Seika, Tokyo, Japan; 5,000 U/kg) was injected into the quadriceps muscle for antibiosis. The rabbits were placed prone on the surgical table and shaved. A dorsal midline skin incision was made and the bilateral transverse processes of L5 and L6 were exposed through the intermuscular plane between the multifidus and longissimus muscles [31]. The transverse processes were

decorticated using an electric burr. Autogenous cortico-cancellous bone was harvested from the iliac crest through extended fascial incisions. In the HA groups, 1.5 ml of cubic shaped HA granules (3–4 mm in width) and an equal amount of morselized autogenous iliac bone were mixed and grafted to the intertransverse space at L5–6 bilaterally. In the Auto group, 3.0 ml of pure autogenous iliac bone was grafted. After irrigation, the fascial incisions were closed with 3-0 absorbable sutures and the skin was closed with 3-0 nylon sutures.

All rabbits were housed one per cage and allowed an ad libitum diet and water. Their neurological conditions and general health were checked each day. At postoperative five weeks, all animals were euthanized with an intravenous administration of sodium pentobarbital (200 mg/kg bolus) and the lumbar spinal segment from L1 to S2 was removed en bloc with the surrounding soft tissue. An operative segment was carefully retrieved and postmortem analyses including biomechanical testing, radiographical and histological evaluations were performed.

Manual palpation and biomechanical testing

The operative segments were gently trimmed off all the soft tissue. Fusion status was assessed according to the magnitude of the flexion-extension motion of the segments by manual palpation [7]. They were graded as fused or not fused by two independent orthopaedists who were blinded to the experimental group of the animal.

All spines were stored in sealed double-plastic bags at –28°C until preparation for testing. Before biomechanical testing, each specimen was completely thawed at room temperature. Each fusion mass was evaluated by non-destructive three-point bending testing using the biomechanical testing machine (858 Mini Bionix II, MTS System Co., Minneapolis, MN, USA) [11]. The schema of biomechanical testing is shown in Fig. 2a. A small jig was designed to hold the motion segment and to allow three-point bending tests at the center of the fused disc space. The adjacent vertebral bodies were placed with their dorsal sides down on two fulcra separated by 25 mm. The upper anvil (7.0 mm in diameter) was placed to apply a load on the ventral surface of the intervertebral disc vertical to the longitudinal spine. A preload of 10 N was applied to the specimen, and the crosshead was zeroed at this point. The specimen was then cyclically preconditioned with 5 cycles to 0.5 mm of deformation at a rate of 0.4 mm/s. A load was applied to 2.0 mm of the deformation at a rate of 0.1 mm/s. The stiffness of the motion segment was defined as the linear slope of the load-displacement curve at 1.5 mm of deformation. Two load-displacement curves were obtained in each specimen, and the average stiffness was used as the representative value. The stiffness of the unsuccessful fusion segments defined by the manual palpation could not be calculated by the three-point bending testing because those segments showed more than 1 mm of deformation under the 10 N of the preload, and therefore the unsuccessful fusion segments were excluded from the three-point bending testing.

Radiographical and histological evaluations

Following mechanical tests, the specimens in each group were subjected to undecalcified tissue processing. The specimens were fixed in 70% ethanol for about 1 week. After fixation, they were dehydrated sequentially in 70, 80, 90 and 100% ethanol and were embedded in polyester resin. Two sections from each specimen were cut with a crystal microtome at a thickness of 500 μm. The cutting lines were parallel to the spinal longitudinal axis at 5 mm from the lateral edge of the intervertebral disc. The schema of cutting lines is shown in Fig. 2b. The sections were

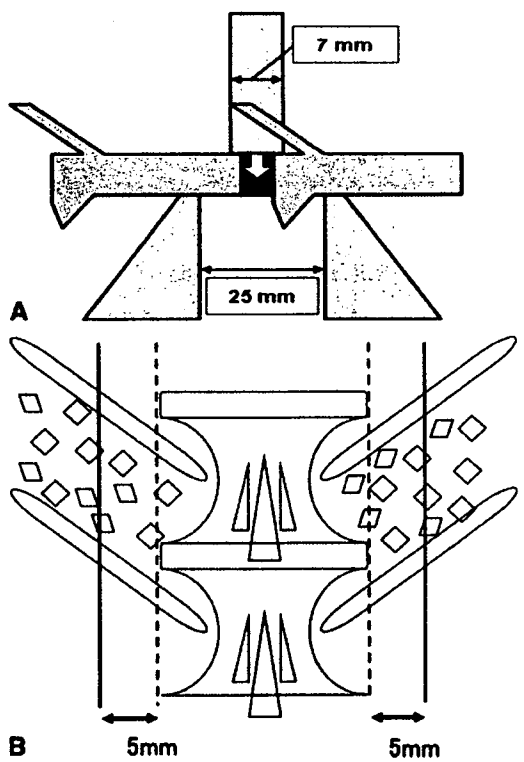

Fig. 2 **a** The schema of the three-point bending test of the operative segment. **b** The schema of the cutting lines for histological section. *Solid lines* indicate cutting lines, and *broken ones* indicate the lateral edges of the intervertebral disc

polished to a thickness of 500–80 μm and observed by contact microradiography (CMR) and light microscopy.

Contact microradiography

The section was mounted on a high-resolution film (SO-181; Kodak Co., Tokyo, Japan) and CMR was taken using a soft X-ray unit (SRO-M50D; Tanaka X-ray MFG. Co. Ltd, Tokyo, Japan) at 14.0 kVp, 2 mA, and an exposure time of 18 min. Newly formed mineralized bone within and around the implanted HA was investigated from the extent of radiographical density.

Histological analyses

After taking CMR, all sections were stained with Toluidine blue O and evaluated with a light microscope. For quantitative analysis, the images of those sections were captured through a light microscope. The mineralized bone area, which had been stained blue purple by Toluidine blue O staining, was then highlighted for measurement. The following parameters were calculated based on the dimensional data measured by "Win roof" software (Mitani Co., Fukui, Japan): bone ingrowth ratio (BIR), bone apposition ratio (BAR), BV/TV, and bone volume ratio outside implant (BV/TV_{out}). Bone ingrowth ratio was determined as the ratio of combined total bone volume within each HA to the combined total pore volume of HA [15]. Bone apposition ratio was the ratio of the combined total length of direct bone bonding to each HA to the combined total length of each HA in fusion mass [22]. BV/TV was measured as a ratio of bone volume within fusion mass, while BV/TV_{out} was measured as a ratio of bone volume within fusion mass outside the implanted granules. The values for each parameter were determined separately for the left and right side fusion mass in each rabbit. Each section was calculated two times by a single observer, and the two values were averaged.

Statistical methods

All parameters were analyzed by analysis of variance (ANOVA). Fusion rates among the groups were compared using Fisher's exact test. The biomechanical and histological evaluations among groups were calculated by ANOVA combined with a Fisher's-protected least-significant difference (Fisher's PLSD) or Bonferroni multiple comparison test when appropriate (StatView, SAS Institute Inc. Cary, NC, USA). The results were expressed as the mean ± standard deviation (SD), and were considered statistically significant at $P < 0.05$.

Results

All rabbits survived the surgery, and ambulated one day later. A total of six animals, including three from the HA15% group, one from the HA50% group, and two from the HA85% group, died from deep wound infections and were excluded from the study. Because of the high incidence of infection in the early series of the animals in this study, the draping and irrigation techniques at the surgical site were modified and the animals were treated with an additional short course of antibiotic therapy in the later series.

Manual palpation and biomechanical testing

The manual palpation test showed that the fusion rates in the three HA groups ranged from 60 to 75% in this PLF model, and there was no significant difference between each HA group. In the Auto group fusion rate was 100%, which was higher than those in the HA groups. However, the difference was not significant (Table 2).

The result of the three-point bending testing showed that the bending stiffness in the HA15% group was lower than those in the other three groups. However, there was no significant difference in the bending stiffness among the four groups (Table 2).

Contact microradiography

CMR photographs in the HA15% group showed that direct bonding between the surface of the HA and the newly mineralized bone was seen in a limited area (Fig. 3a). In the HA50% group, there was also only a little direct bone bonding with the implant and bone ingrowth could be seen only in peripheral pores of the HA granule (Fig. 3b). On the other hand, the newly mineralized bone formed deeply inside the HA85% granules and bonded directly with the implanted materials in the fusion mass. The newly formed bone inside the HA85% remained connected to the bone tissue outside the material (Fig. 3c). High magnification

Table 2 Fusion rate and bending stiffness of fusion mass

Group	Number (%) of fused specimen	Bending stiffness (N/mm)
HA15%	5/8 (62.5)	99.3 ± 52.0
HA50%	6/8 (75.0)	127 ± 2.0
HA85%	5/8 (62.5)	122 ± 47.5
Auto	6/6 (100)	123 ± 38.6

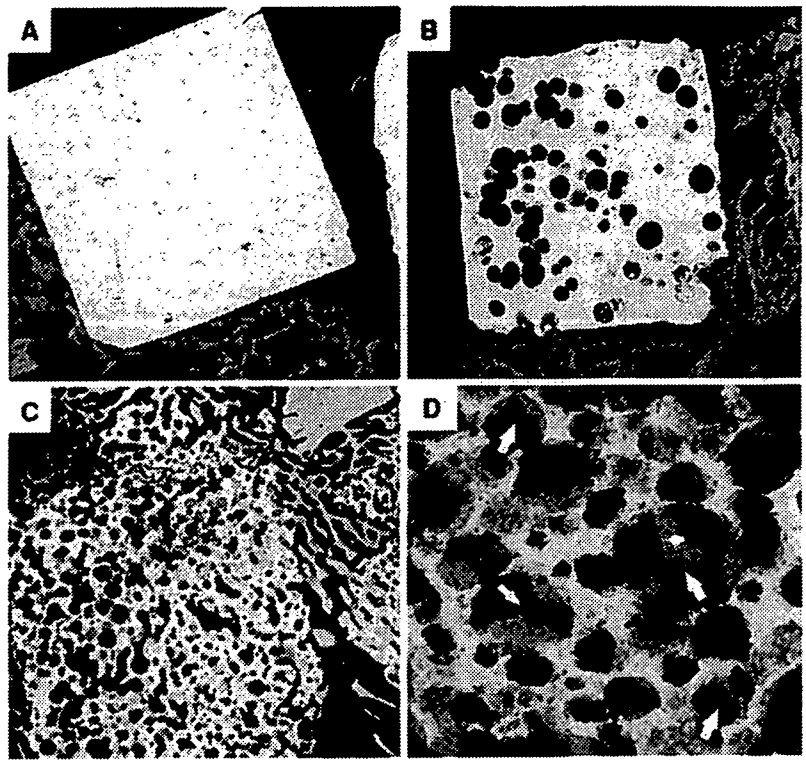

Fig. 3 Contact microradiographs of the sagittal section of the fusion mass containing the HA granules. In the HA15% group (**a**) and HA50% group (**b**), there is only a little direct bonding between the HA granules (*white*) and the newly mineralized bone (*gray*). On the other hand, in the HA85% group (**c**, **d**), there is excellent unification between the HA (*white*) and newly mineralized bone (*gray*). *Arrows* show newly mineralized bone within pores of the HA85% granule (magnification: **a**–**c** ×5, **d** ×30)

photographs showed an excellent unification between the HA and the newly trabecular bone (Fig. 3d).

Histological analyses

In histological findings of the Auto group, both bone and cartilage formation could be seen at the intertransverse space of L5–6. The grafted bone was integrated with the newly formed trabecular bone within the fusion mass at 5 weeks after implantation (Fig. 4a).

Distinct histological differences were observed among the HA groups. In the HA15% and HA50% groups, microphotographs showed that bone ingrowth could be seen only in peripheral pores of the HA granules and its surface was mainly covered with fibrous tissue or empty space (Fig. 4b, c, e, f). Although bridging bone was formed between the L5 and L6 transverse process in these specimens, there was only a little direct bone bonding with the HA granules. On the other hand, in the HA85% group, bone ingrowth was achieved throughout the HA granules via the interconnecting pores and the amount of direct bone bonding area was the largest among the three HA groups (Fig. 4d, g). The HA85% was integrated with the newly formed bone in the fusion mass. Middle magnification microphotographs in the HA85% group showed that the newly formed bone covered the microporous surface of macropores inside the material (Fig. 4h). High magnification microphotographs in the HA85% also showed the presence of osteoblast-like cells attached to the rough surface of macropores (Fig. 4i).

Quantitative histological evaluation showed that the average BIR was the highest in the HA85% group (24.0%), and lower in the HA15% (0%) and the HA50% groups (2.0%) (Fig. 5a). The average BAR in the HA85% group (14.3%) was also superior to those in the HA15% (4.8%) and the HA50% group (6.2%) with a statistical significance (Fig. 5b). The average BV/TV were 19.4, 22.4, 24.5, and 40.6% in the HA15%, HA50%, HA85%, and the Auto groups, respectively (Fig. 5c). The average BV/TV_{out} were 26.9, 31.9, and 30.8% in the HA15%, HA50%, and HA85% groups respectively (Fig. 5d). The Auto group showed the highest BV/TV among the four groups, which was statistically significant (Fig. 5c). While, there was no statistically significant difference among the three HA groups in the BV/TV_{out} (Fig. 5d).

Discussion

Owing to the progress in production methods of HA, HA can now be controlled in its porosity and even in the dimensions of the pores themselves through manufacturing processes. Many researchers have reported that porous modifications of HA achieved successful healing outcomes in various sites such as metaphyseal bone defects. However, there have been few studies related to the significance

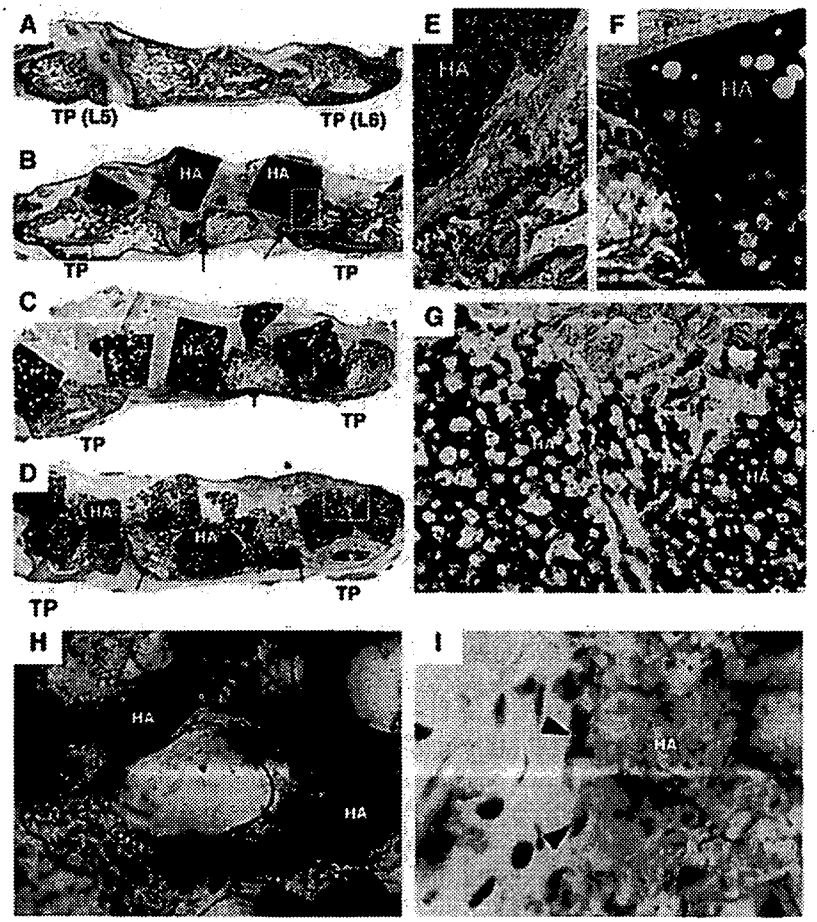

Fig. 4 Histological sagittal sections of the fusion mass stained with Toluidine Blue O in a rabbit PLF model (**a–i**). In the Auto (**a**) group, both bone (**b**) and cartilage (**c**) formation can be seen between the L5 and L6 transverse process (*TP*). In the HA15% (**b, e**) and the HA50% (**c, f**) group, newly formed bone (*arrows*) can be seen between the L5 and L6 transverse process. However, there is only a little direct bone bonding with the HA granules. In these specimens, most surfaces of the HA granules are surrounded by fibrous tissue (**f**), and bone ingrowth is obtained only in peripheral pores of the implanted HA. In the HA85% (**d, g**) group, newly formed bone integrates with the HA granules and bone ingrowth is achieved throughout the materials. High magnification photographs in the HA85% (**h, i**) group show newly formed bone (*blue–purple*) covers the microporous surface in each macropore of HA (*brown*) and many osteoblast-like cells (*arrowheads*) are seen attached to the rough surface of the HA (magnification: **a–d** ×1, **e–g** ×5, **h** ×50, **i** ×250)

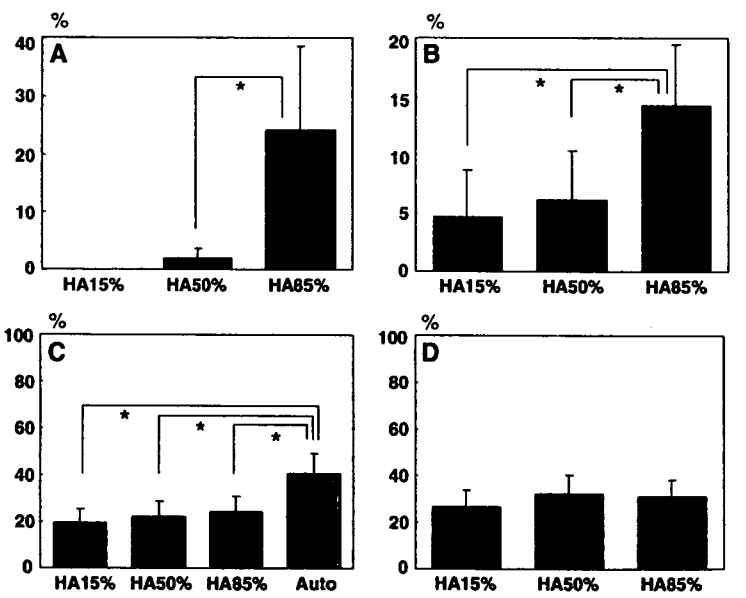

Fig. 5 The results of quantitative histological analysis of the fusion mass. The bone ingrowth rate (*BIR*) (**a**) and the bone apposition rate (*BAR*) (**b**) are higher in the HA85% group compared to those in the HA15% and HA50% group. In contrast, there is no significant difference among the three HA groups in the bone volume rate outside the implanted granules (BV/TV_{out}) (**d**), although it is significantly higher in the Auto group than any other groups in the bone volume rate (BV/TV) (**c**). (mean ± SD, * $P < 0.05$)

of HA porous structure in PLF. In the current study, we hypothesized that HA porous characteristics also had an influence on healing outcomes in PLF. We investigated this hypothesis using three types of HA with different porosities as a bone graft extender in a rabbit PLF model.

The histological results of this study showed the superiority of the HA85% in both osteoconduction and osteointegration compared to the HA15% and HA50% in a rabbit PLF model, although there was no significant difference in fusion rate and mechanical strength between the three HA groups. We believe that this superiority of the HA85% derives not only from the high porosity but also from the abundant interconnecting pores. This is because the interconnected porous structure has been reported to be the most important for osteoconduction and osteointegration among various porous parameters [1, 29]. Since cell migration, mineralization, and subsequent bone remodeling depend on vessel ingrowth, the vascularization through the interconnecting pores is indispensable for bone ingrowth and for maintaining cellular viability in the material. In the HA85% group there were abundant osteogenic cells and mineralized trabecular bone throughout the implanted granules at five weeks after implantation in this PLF model. We observed that the newly formed bone inside the materials remained connected to the bone tissue outside them via the interconnecting pores. In addition, few differences in the histological results between the HA15% and the HA50% indicate that the porous interconnection of HA is more important than its porosity in PLF. On the basis of these results, we reasonably conclude that the interconnecting pores of HA also have a significant influence on the healing outcomes in the environment of PLF.

Moreover, the microporous structure in every macropore possibly contributed to the excellent histological outcomes in the HA85% group, although its effect on the behavior of bone healing is still controversial. Some researchers reported that the micropores (<10 μm in diameter) would not be permissive to osteoconduction because the size of the nucleus in most mammalian cells is more than 10 μm [24, 29]. On the other hand, Annaz et al. [2] reported that the microporous surface played a role in initial cellular anchorage and attachment of osteogenic cells [14]. Habibovic et al. demonstrated that modification of the microporous surface affected the interface dynamics of the ceramic in such a way that relevant cells were triggered to differentiate into the osteogenic lineage [12, 13, 25, 34]. After 5 weeks implantation, many osteoblast-like cells were settled on the microporous surface of macropores within the HA85% granules, and the newly formed bone covered the rough surface of the material. The current study did not prove directly the significance of the microporous structure, but this data may support the idea that the microporous modification within each macropore is beneficial for osteoconduction and osteointegration in PLF.

From the distinct histological difference among three HA groups, there may be a fundamental difference between the non-interconnected porous HA and the interconnected porous HA in the role as bone graft extenders in PLF. The non-interconnected porous HA did not integrate with newly formed bone even in fusion mass which obtained solidity. This result indicates that the non-interconnected porous HA works only as a space maintainer and that the newly formed bone around the HA granules plays a role in stabilizing the operative segment. The implanted HA without osteointegration will obstruct bone remodeling in fusion mass, and will result in heterogeneous bone tissue [23]. On the other hand, the interconnected porous HA85% granules obtained an excellent unification with the newly mineralized bone in fusion mass. Despite the existence of the HA granules, the fusion mass consisted of a relatively homogenous trabecular structure. In other words, the HA85% works as a scaffold for newly formed bone, and the trabecular bone both inside and outside the HA granules firmly connect each other to provide structural support in PLF.

On the contrary to the histological results, the porous modification of HA has little influence on fusion rate and mechanical strength in this PLF model. In an environment of metaphyseal bone defect, the interconnected high porous HA could obtain excellent mechanical outcomes in correlation with bone ingrowth within materials as previously reported [29]. However, the histological superiority of BIR and BAR in the HA85% group was not consistent with that of the fusion rate and mechanical strength in this PLF model. This is probably because primary stabilization of the fusion segment may be achieved by bridging bone between the adjacent transverse processes outside the implanted materials, rather than the degree of integration between the newly formed bone and the granules in PLF. This speculation is supported by our result that there was no difference either in BV/TV_{out} and/or fusion rate between the three HA groups, whereas the higher fusion rate in the Auto group will be consistent with the higher BV/TV. We believe that porous modification of HA only is insufficient to promote bone formation outside materials in PLF because HA does not have the ability of osteoinduction.

Despite the superiority of the HA85% in osteoconduction and osteointegration, a high porous material is always accompanied by a problem of fragility as a bone graft substitute. Initial compressive strength of the HA85% is only 2.0 MPa, which is equivalent to cancellous bone, but failure of the granules could not be seen in this PLF model. This is because the environment of a grafted site in PLF is initially non-weight bearing and fusion mass gradually

begins to play a role in load-transmission with its maturation [17]. Therefore, bone graft substitutes in PLF mainly require the capability for bone formation rather than initial mechanical strength. It is supposed that the interconnected high porous HA would be a rational material for a bone graft extender in PLF.

The current study includes some potential design limitations. First, the bone healing capability of rabbits is much higher than that of humans as previously reported [4] and therefore, all the findings of this study might not be applicable to clinical PLF. Benefits of superior osteointegration ability of the HA85% to the non-interconnected porous HAs became obscure by rapid bridging bone formation outside the implant in this rabbit model, however, the findings that the porous modifications of HA had little influence on primary stabilization of the fusion segment is possibly true of clinical PLF. Because bridging bone generated by autogenous bone graft is more easily and rapidly achieved than bone ingrowth to the implanted HA, it seems reasonable to suppose that bridging bone formation through the interval between the HA granules precedes the bone ingrowth to the HA when HA is used as a bone graft extender even in clinical PLF. Second, we carried out the evaluations only at 5 weeks. Because Boden et al. [5, 6] reported that if solid fusion was not seen after 5 weeks, assessment at longer time points did not show an increase in the fusion rate or the biomechanical properties of the fusion mass in this rabbit PLF model. Since the fusion mass in the Auto group obtained solidity at 5 weeks in our results, this time point seemed to allow the adequate evaluation of the mechanical outcomes in this model. However, long-term effects of HA porous characteristics on the histological outcomes must be examined. Finally, we should also pay attention to the influence of HA granule size on healing outcomes especially in the non-interconnected porous HA groups. Because of few interconnecting pores, the fusion mass would gradually become more heterogeneous as the granule size of the non-interconnected porous HA increases.

The current study demonstrated that the HA porous characteristics had an effect on the histological outcomes in a rabbit PLF model. The interconnected high porous structure seems to be promising for the environment of PLF in the point of producing fusion mass with higher cellular viability. This is because the HA85% is superior in terms of integration with the newly formed bone in fusion mass compared to the non-interconnected porous HAs. However, the porous modifications of HA have little influence on fusion rate and mechanical strength because primary stabilization of the fusion segment is mainly achieved by bridging bone between the adjacent transverse processes outside the implanted materials, rather than the degree of integration between the newly formed bone and the HA granules in PLF.

Acknowledgments The authors would like to acknowledge Michiko Sakamoto, B.S., PENTAX Co., for their technical support and for providing materials. They are also grateful to Mr. Justin Collings for correcting their use of language. This study was supported by PENTAX Co.

References

1. Akazawa T, Murata M, Sasaki T (2006) Biodegradation and bioabsorption innovation of the functionally graded bovine bone-originated apatite with blood permeability. J Biomed Mater Res A 76(1):44–51
2. Annaz B, Hing KA, Kayser M (2004) Porosity variation in Hydroxyapatite and Osteoblast morphology: a scanning electron microscopy study. J Microsc 215(Pt 1):100–110
3. Berven S, Tay BK, Kleinstueck FS (2001) Clinical applications of bone graft substitutes in spine surgery: consideration of mineralized and demineralized preparations and growth factor supplementation. Eur Spine J 10(Suppl 2):S169–S177
4. Boden SD (2002) Overview of the biology of Lumbar spine fusion and principles for selecting a bone graft substitute. Spine 27(16 Suppl 1):S26–S31
5. Boden SD, Martin GJ Jr, Morone M (1999) The use of Coralline Hydroxyapatite with bone marrow, autogenous bone graft, or osteoinductive bone protein extract for posterolateral Lumbar spine fusion. Spine 24(4):320–327
6. Boden SD, Schimandle JH, Hutton WC (1995) 1995 Volvo Award in basic sciences. The use of an osteoinductive growth factor for lumbar spinal fusion. Part Ii: Study of dose, carrier, and species. Spine 20(24):2633–2644
7. Boden SD, Schimandle JH, Hutton WC (1995) An experimental lumbar intertransverse process spinal fusion model. Radiographic, histologic, and biomechanical healing characteristics. Spine 20(4):412–420
8. Chang BS, Lee CK, Hong KS (2000) Osteoconduction at porous hydroxyapatite with various pore configurations. Biomaterials 21(12):1291–1298
9. Flautre B, Descamps M, Delecourt C (2001) Porous ha ceramic for bone replacement: role of the pores and interconnections—experimental study in the rabbit. J Mater Sci Mater Med 12(8):679–682
10. Fujishiro T, Nishikawa T, Niikura T (2005) Impaction bone grafting with hydroxyapatite: increased femoral component stability in experiments using sawbones. Acta Orthop 76(4):550–554
11. Glazer PA, Heilmann MR, Lotz JC (1997) Use of electromagnetic fields in a spinal fusion. A rabbit model. Spine 22(20):2351–2356
12. Habibovic P, Yuan H, van der Valk CM (2005) 3D Microenvironment as essential element for osteoinduction by biomaterials. Biomaterials 26(17):3565–3575
13. Hing KA (2004) Bone repair in the twenty-first century: biology, chemistry or engineering? Philos Transact A Math Phys Eng Sci 362(1825):2821–2850
14. Hing KA, Annaz B, Saeed S (2005) Microporosity enhances bioactivity of synthetic bone graft substitutes. J Mater Sci Mater Med 16(5):467–475
15. Hing KA, Best SM, Tanner KE (2004) Mediation of bone ingrowth in porous hydroxyapatite bone graft substitutes. J Biomed Mater Res A 68(1):187–200
16. Ito M, Kotani Y, Hojo N, (2007) Effects of porosity changes in hydroxyapatite ceramics vertebral spacer on its binding capability to the vertebral body: an experimental sheep study. J Neurosurg 6(5):431–437